Reduction of the Lamina Cribrosa Curvature After Trabeculectomy in Glaucoma

Seung Hyen Lee,[1] Da-Ae Yu,[2] Tae-Woo Kim,[1] Eun Ji Lee,[1] Michaël J. A. Girard,[3,4] and Jean Martial Mari[5]

[1]Department of Ophthalmology, Seoul National University College of Medicine, Seoul National University Bundang Hospital, Seongnam, Korea
[2]Seoul National University College of Medicine, Seoul, Korea
[3]Department of Biomedical Engineering, National University of Singapore, Singapore
[4]Singapore Eye Research Institute, Singapore National Eye Centre, Singapore
[5]GePaSud, Université de la Polynésie Française, Tahiti, French Polynesia

Correspondence: Tae-Woo Kim, Department of Ophthalmology, Seoul National University Bundang Hospital, 82, Gumi-ro, 173 Beon-gil, Bundang-gu, Seongnam, Gyeonggi-do 463-707, Korea; twkim7@snu.ac.kr.
Eun Ji Lee, Department of Ophthalmology, Seoul National University Bundang Hospital, 82, Gumi-ro, 173 Beon-gil, Bundang-gu, Seongnam, Gyeonggi-do 463-707, Korea; opticdisc@gmail.com.

Submitted: December 18, 2015
Accepted: August 11, 2016

Citation: Lee SH, Yu D-A, Kim T-W, Lee EJ, Girard MJA, Mari JM. Reduction of the lamina cribrosa curvature after trabeculectomy in glaucoma. *Invest Ophthalmol Vis Sci*. 2016;57:5006–5014. DOI:10.1167/iovs.15-18982

Purpose. To investigate whether the lamina cribrosa (LC) curvature is decreased after trabeculectomy.

Methods. Thirty-nine eyes of 39 patients with primary open-angle glaucoma who underwent trabeculectomy were included. Optic nerves were scanned by using enhanced-depth-imaging spectral-domain optical coherence tomography before and after trabeculectomy. The LC curvature was assessed by measuring the LC curvature index (LCCI) in seven horizontal B-scan images in each eye.

Results. The LCCI was significantly smaller at postoperative 6 months than at the preoperative level in all seven planes (all $P < 0.001$). Preoperative LCCI was associated with younger age at superior midperiphery, midhorizontal plane, inferior midperiphery (all $P \leq 0.005$) and higher preoperative intraocular pressure (IOP) at superior and inferior midperiphery (both $P = 0.039$). Younger age and larger preoperative LCCI were associated with a larger reduction of the LCCI at all three locations ($P = 0.003$ and 0.031 at superior midperiphery, $P = 0.011$ and 0.001 at midhorizontal plane, and $P = 0.014$ and 0.005 at inferior midperiphery, respectively), whereas the percentage IOP lowering was associated at superior and inferior midperiphery ($P = 0.017$ and 0.047, respectively).

Conclusions. Lamina cribrosa curvature was reduced after trabeculectomy. This finding suggests that LC curvature may have value as a parameter relevant to optic nerve head biomechanics.

Keywords: lamina cribrosa, curvature, trabeculectomy, optic nerve head, reduction

The glaucomas are a group of disorders that are characterized by loss of retinal ganglion cells and their axons, and corresponding visual field defects. Although IOP-related stress is the most important risk factor,[1,2] the following clinical observations have led to the proposal of other factors being important in the development and progression of glaucomatous optic neuropathy: (1) glaucoma does not always develop in eyes with ocular hypertension,[3–5] (2) glaucoma can develop in eyes with IOP within statistically normal limits,[6] and (3) glaucoma often progresses despite considerable lowering of IOP.[7] Glaucoma patients are currently uniformly treated by lowering the IOP.

Currently, there is no method to identify whether a patient's disease is mainly attributed to IOP-induced mechanical stress or non–IOP-related factors. A high or low IOP per se cannot be an indicator for the presence or absence of clinically meaningful mechanical stress/strain within the optic nerve head (ONH), since a high IOP does not always induce glaucomatous optic neuropathy.[3] In contrast, computational modeling studies[2,8] suggest that the ONH can be subjected to substantial mechanical stress even when the IOP is within its normal limits. The ability to stratify this disease according to IOP-induced mechanical stress as a causative factor would help toward the development of tailored treatment strategies.

Histologic studies have postulated that posterior bowing of the lamina cribrosa (LC) is a primary pathogenic event in glaucoma when IOP-induced mechanical stress is transferred to the ONH.[9] Lamina cribrosa bowing would in turn affect the axons passing through the laminar pores,[10–12] which may lead to direct axonal damage, or indirect damage through the interruption of the axoplasmic flow, alteration in the microcapillary blood flow, or activation of astrocytes, glial, and LC cells.[2,13,14] Accordingly, a proper characterization of ONH biomechanics in vivo may be a necessary step toward an improved understanding of glaucoma pathogenesis.[15,16] So far, parameters that are related to the biomechanics of the ONH and measurable in vivo have been limited. While LC depth measured from the Bruch's membrane opening (BMO) level has been examined as a parameter that represents the anteroposterior LC position,[17–21] it cannot directly represent the strain of the LC. This is because LC depth can be significantly influenced by the choroidal thickness, which is known to be variable among individuals.[22] For instance, the LC depth would be measured as large in eyes with thick peripapillary choroid even

if the anterior surface of the LC remains at its original position without any deformation.

We postulated that LC curvature may be a clinically meaningful parameter for evaluating the LC strain, since its measurement is not influenced by the choroidal thickness. However, LC curvature should have a tendency to be flat or slightly curved as long as a high translaminar pressure difference (TLPD) is not imposed. Otherwise, a large LC curvature may be simply a reflection of interindividual variation.

The purpose of the current study was to investigate whether LC curvature is reduced after IOP lowering in eyes with primary open-angle glaucoma (POAG). Although it has already been demonstrated that the LC depth may be reduced by IOP lowering,[18,20] whether the LC curvature varies in accordance with IOP lowering remains to be determined. The factors influencing the change in LC curvature were also investigated.

Methods

This investigation was based on ongoing prospective investigations of glaucoma patients at the Seoul National University Bundang Hospital Glaucoma Clinic: the Lamina Cribrosa Exploration Study[23,24] and the Investigating Glaucoma Progression Study.[25,26] Both of these studies involved consecutive subjects who met the eligibility criteria and provided written informed consent to participate. This study was approved by the Seoul National University Bundang Hospital Institutional Review Board and conformed to the Declaration of Helsinki.

Study Subjects

Before the study, each patient underwent a complete ophthalmic examination including visual acuity assessment, refraction, slit-lamp biomicroscopy, gonioscopy, Goldmann applanation tonometry, and dilated stereoscopic examination of the optic disc, as well as measurement of corneal curvature (KR-1800; Topcon, Tokyo, Japan), central corneal thickness (Orbscan II; Bausch & Lomb Surgical, Rochester, NY, USA), and axial length (IOL Master version 5; Carl Zeiss Meditec, Dublin, CA, USA), and stereo disc photography (EOS D60 digital camera; Canon, Utsunomiya-shi, Tochigi-ken, Japan), spectral-domain optical coherence tomography (SD-OCT, Spectralis OCT; Heidelberg Engineering, Heidelberg, Germany), and standard automated perimetry (Humphrey Field Analyzer II 750 and 24-2 Swedish interactive threshold algorithm; Carl Zeiss Meditec).

The inclusion criteria for the subjects were having POAG, a best-corrected visual acuity of at least 20/40, a spherical refraction of −8.0 to +3.0 diopters, and a cylinder correction within ±3.0 diopters. Primary open-angle glaucoma was defined as the presence of glaucomatous optic nerve damage (i.e., the presence of focal thinning, notching, or a splinter hemorrhage) and associated visual field defect without ocular diseases or conditions that may elevate the IOP. A glaucomatous visual field change was defined as (1) outside the normal limit on the glaucoma hemifield test, (2) three abnormal points with a $P < 5\%$ probability of being normal, one point with $P < 1\%$ by pattern deviation, or (3) a pattern standard deviation of $P < 5\%$ confirmed on two consecutive reliable tests. A visual field measurement was considered as reliable when both false-positive and false-negative results were <25% and fixation losses were <20%.

Those with a history of previous intraocular surgery or coexisting retinal (e.g., diabetic retinopathy, retinal vessel occlusion, or retinoschisis) or neurologic diseases (e.g., pituitary tumor) that could affect the visual field were excluded from this study. Secondary glaucoma (e.g., uveitic glaucoma) that may increase IOP was also excluded. Eyes were also excluded when a good-quality image (i.e., quality score > 15) could not be obtained in more than five sections, the quality score did not reach 15, the image-acquisition process automatically stopped, or images of the respective sections were not obtained. Eyes with tilted disc, and signs of hypotony, maculopathy, or disc edema after surgery were also excluded.[27]

Indications for surgical treatment (trabeculectomy) were IOP deemed to be associated with a high risk of progression or glaucomatous progression of the visual field or optic disc, despite taking the maximum tolerated medications. All ocular hypotensive medications were continued up to the time of surgery. The preoperative IOP was defined as the average of two measurements made within 2 weeks before trabeculectomy.

Optic discs were examined by using SD-OCT at 1 day before surgery and 6 months postoperatively. Intraocular pressure measurements made by using Goldmann applanation tonometry were recorded at the follow-up visit.

Enhanced-Depth-Imaging OCT of the Optic Nerve Head

The optic nerve was imaged by using the enhanced-depth-imaging technique of the Spectralis OCT system. This technique was originally developed by Spaide et al.[28] to visualize the full thickness of the choroid. This technique yields images with a stronger signal and better image contrast in the deep ONH tissue, compared to the conventional imaging technique.[24] Patients were imaged through undilated pupils by using a rectangle subtending $10^\circ \times 15^\circ$ of the optic disc. This rectangle was scanned with approximately 75 B-scan section images that were separated by 30 to 34 μm (the scan line distance was determined automatically by the machine). Approximately 42 SD-OCT frames were averaged for each section. This protocol provided the best trade-off between image quality and patient cooperation.[24] Potential magnification errors were avoided by entering the corneal curvature of each eye into the Spectralis OCT system before scanning.

Quantification of Posterior Bowing of the LC

To quantify the posterior bowing of LC on the SD-OCT B-scan images, we defined the lamina cribrosa curvature index (LCCI) as the inflection of a curve representing a section of the LC. The LCCI was determined by first measuring the width of BMO (W) and then measuring the LC curve depth (LCCD) within the BMO in each B-scan (Fig. 1). The BMO width (W) was defined as the distance between the temporal and nasal termination point. Lines were drawn from each BM termination point perpendicular to the BMO reference line, until they met the anterior LC surface. The line connecting the two points on the anterior LC surface was used as the reference line to measure the LCCD, which was defined as the maximum LC depth from the reference line (Fig. 1). The LCCI was then calculated as $(LCCD/W) \times 100$. Since the curvature was thereby normalized according to LC width, it describes the shape of the LC independent of the actual size of the ONH. Specifically, $(LCCD/W) \times 100$ is a simple normalized measure that represents the posterior bowing or curvature of the anterior LC surface within the BMO. Only the LC within the BMO was considered because the LC was often not clearly visible outside of the BMO.

Before the measurement, the visibility of the peripheral LC was enhanced by postprocessing images by using adaptive compensation (Fig. 1).[29,30] Measurement was performed by

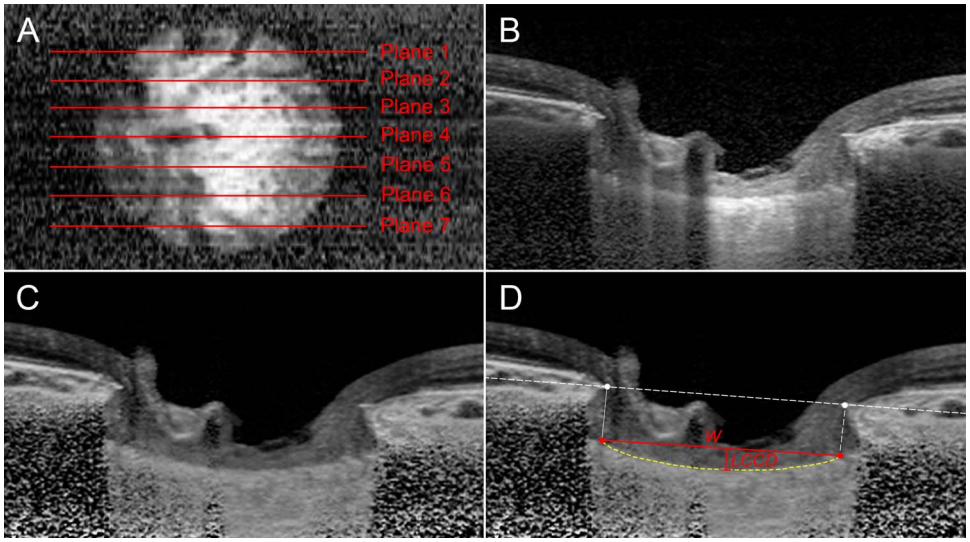

Figure 1. Measurement of the LCCI. (**A**) En face image generated from a volume scan of the optic nerve head. (**B**) B-scan image obtained at plane 4 as shown in (**A**). (**C**) Same image as in (**B**) postprocessed by adaptive compensation. (**D**) The LCCI was measured by dividing the LCCD within the BMO by the BMO width (*W*), and then multiplying by 100.

using a manual caliper tool in the Amira software (version 5.2.2; Visage Imaging, Berlin, Germany) at seven selected B-scan images spaced equidistantly across the vertical optic disc diameter in each eye. These seven B-scan lines were defined as planes 1 to 7 (top to bottom in Fig. 1), where plane 4 corresponds to the midhorizontal plane, and planes 2 and 6 correspond to the superior and inferior midperiphery, respectively.

The LCCI was measured on preoperative B-scan images and postoperative 6-month follow-up B-scan images. For the follow-up measurement, the B-scan images were selected to correspond with those that had been selected for the baseline measurements by using the en face images and the low reflective shadow within the LC to confirm the correspondence of the B-scan image series between the two time points.

The LCCIs were measured by two experienced observers (SHL and EJL) who were masked to the clinical information. The average of the measurements from each of the two observers was used for analysis.

Statistical Analysis

The interobserver agreement for measuring the LCCI was evaluated by calculating the 95% limits of agreement according to Bland-Altman. The pre- and postoperative amounts of LCCI, LCCD, and BMO width were compared by using the paired *t*-test. The degree of reduction in the LCCI was compared between adjacent planes by using repeated-measures ANOVA. Regression analysis was used to investigate the factors associated with the preoperative LCCI and the amount of reversal of this curvature, first with a univariate model and then with a multivariate model that included variables from the univariate model for which $P < 0.10$. This analysis was performed for the superior midperipheral, midhorizontal, and inferior midperipheral planes (planes 2, 4, and 6, respectively). Statistical analyses were performed by using the Statistical Package for the Social Sciences software (version 22.0; SPSS, Chicago, IL, USA). Probability values of $P < 0.05$ were considered indicative of statistical significance. Except where stated otherwise, the data are presented as mean ± SD values.

Results

Baseline Characteristics

Fifty-one patients with POAG who underwent trabeculectomy were initially included. Of these, 12 were excluded owing to poor scan image quality (>5 missing sections in an average of 75 sections). The LC, especially its anterior surface, was readily discernible in most of the B-scan images at both the pre- and postoperative examinations in the remaining 39 patients.

The patients were 51.5 ± 18.4 years old (range, 15–85 years), and 16 (41%) were women. The entire cohort had a visual acuity ranging from 20/40 to 20/20, a refractive error (spherical equivalent) of −2.36 ± 2.99 diopters (range, −7.25 to +2.75 diopters), and a visual field mean deviation of −13.85 ± 11.49 dB (range, −31.79 to 0.83 dB). The IOP decreased from 27.5 ± 8.9 mm Hg (range, 13–47 mm Hg) to 9.8 ± 3.6 mm Hg (range, 5–16 mm Hg; Table 1) at postoperative 6 months. Before surgery, all patients were using ocular hypotensive medications. At the time of postoperative OCT scan, 13 patients (33.3%) were under medical treatment.

The 95% Bland-Altman limit for interobserver agreement of measuring the 546 values for pre- and postoperative LCCI at the 273 locations (39 eyes × 7 B-scans) was −1.60 to 1.57. Both the LCCI and LCCD decreased significantly in all seven planes

Table 1. Demographic Characteristics of Patients ($n = 39$)

Variables	Mean ± Standard Deviation
Age, y*	51.5 ± 18.4
Male/female	23/16
Spherical equivalent, D*	−2.36 ± 2.99
Preoperative IOP, mm Hg*	27.5 ± 8.9
Postoperative IOP, mm Hg*	9.8 ± 3.6
Axial length, mm*	24.87 ± 0.99
Central corneal thickness, μm*	557.2 ± 57.4
Visual field MD, dB*	−13.85 ± 11.49
Visual field PSD, dB*	7.21 ± 4.29
Global RNFL thickness, μm*	59.6 ± 15.0

D, diopters; IOP, intraocular pressure; MD, mean deviation; PSD, pattern standard deviation; RNFL, retinal nerve fiber layer.

* Values are shown in mean ± standard deviation.

Table 2. Pre- and Postoperative (6-Months) Measurements of the LCCI and LCCD

	LCCI				LCCD, μm		
Plane No.	Preoperative	Postoperative	*P* Value	Reduction of LCCI	Preoperative	Postoperative	*P* Value
1	14.25 ± 2.73	10.55 ± 2.32	**<0.001**	3.70 ± 1.87	174.0 ± 59.5	119.9 ± 35.9	**<0.001**
2	14.42 ± 2.89	10.38 ± 2.07	**<0.001**	4.04 ± 2.30	193.2 ± 70.5	131.3 ± 35.6	**<0.001**
3	13.95 ± 3.34	10.33 ± 2.62	**<0.001**	3.62 ± 2.24	204.0 ± 66.8	141.7 ± 38.4	**<0.001**
4	12.73 ± 2.55	9.96 ± 2.12	**<0.001**	2.77 ± 1.76	193.6 ± 55.7	138.8 ± 25.5	**<0.001**
5	14.39 ± 3.00	10.48 ± 2.23	**<0.001**	3.92 ± 2.18	210.7 ± 66.8	140.5 ± 33.9	**<0.001**
6	14.70 ± 3.43	10.57 ± 2.49	**<0.001**	4.13 ± 2.14	195.7 ± 77.5	131.3 ± 41.5	**<0.001**
7	14.65 ± 2.87	10.90 ± 2.53	**<0.001**	3.75 ± 1.96	173.1 ± 64.0	117.1 ± 34.6	**<0.001**
Average (range)	14.21 ± 2.63 (10.31–20.44)	10.50 ± 1.94 (7.30–13.47)	**<0.001**	3.71 ± 1.82	192.6 ± 61.2 (114.14–448.43)	131.7 ± 28.9 (88.86–257.86)	**<0.001**

All data are shown in mean ± standard deviation. Values with statistical significance are in boldface. LCCI, lamina cribrosa curvature index; LCCD, lamina cribrosa curve depth.

postoperatively (all $P < 0.001$; Table 2), and the change of LCCI was significantly smaller in the midhorizontal plane than in all other planes (Fig. 2). The pre- and postoperative average LCCI at the seven planes ranged from 10.31 to 20.44, and from 7.30 to 13.47, respectively.

In 13 patients the LC was visible up to its insertion to the parapapillary sclera in at least three planes. The LCCI measured over the entire structure (i.e., insertion to insertion) in the 39 (3×13) selected planes was comparable to that of the LCCI measured from the LC within the BMO (10.88 ± 1.90 vs. 10.45 ± 1.93, $P = 0.317$, paired *t*-test). Representative LCCI measurements using the entire LC are shown in Figure 3.

Factors Associated With the Preoperative LCCI

The factors affecting preoperative LCCI were determined by using linear regression analysis. In the univariate analysis, a younger age and higher preoperative IOP ($P < 0.001$ and 0.009 at superior midperiphery, $P = 0.001$ and 0.014 at midhorizontal, $P = 0.001$ and 0.010 at inferior midperiphery) were associated with larger preoperative LCCI (Table 3). Multivariate analysis revealed that younger age and higher preoperative IOP were significant factors affecting the preoperative LCCI in all three regions (all $P \leq 0.005$) and in the superior and inferior midperiphery regions (both $P = 0.039$), respectively (Fig. 4; Table 3).

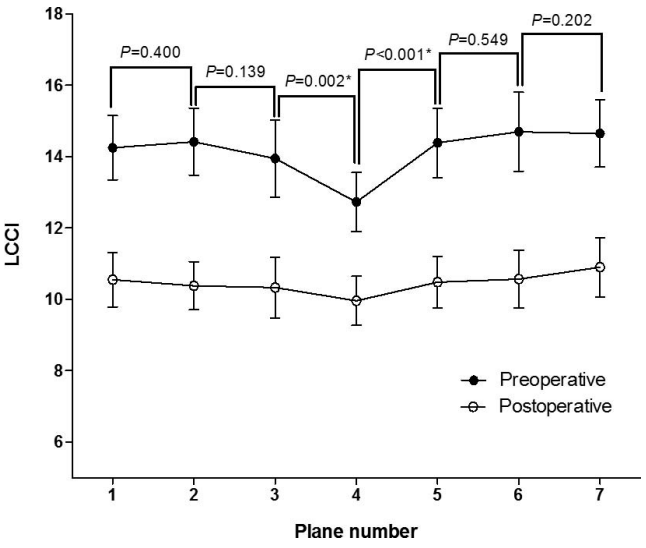

Figure 2. Graph showing the variation in the change in LCCI among the different planes. The change in LCCI was smallest at the midhorizontal plane (plane 4). The *P* values are for the comparison of the LCCI reduction between adjacent planes (repeated-measures ANOVA). *$P < 0.05$.

Factors Associated With Reduction of the LCCI

Univariate analysis revealed that the factors affecting the reduction of the LCCI at the superior and inferior midperiphery and the midhorizontal plane were a younger age ($P < 0.001$ at all three locations), a higher preoperative IOP ($P = 0.003$ at superior and inferior midperiphery, $P = 0.016$ at midhorizontal plane), a larger percentage IOP reduction ($P \leq 0.001$ at superior and inferior midperiphery, $P = 0.005$ at midhorizontal plane), and a larger preoperative LCCI ($P < 0.001$ at all three locations; Fig. 4, Table 4). Preoperative BMO width was associated with the reduction of the LCCI in the midhorizontal plane ($P = 0.048$). Multivariate analysis revealed that younger age and greater preoperative LCCI ($P = 0.003$ and 0.031 at superior midperiphery, $P = 0.011$ and 0.001 at midhorizontal plane, $P = 0.014$ and 0.005 at inferior midperiphery) were significant factors associated with the reversal of the LCCI (Table 4). In addition, the greater percentage IOP reduction was found to be a factor related with the larger reversal of the LCCI in the superior and inferior midperiphery ($P = 0.017$ and 0.047, respectively).

Factors Associated With Preoperative LCCD and Reduction of the LCCD

Younger age ($P = 0.001$) and larger preoperative BMO width ($P < 0.001$) were significantly associated with larger preoperative average LCCD both in the univariate and multivariate analysis (Table 5).

Univariate analysis revealed that a younger age ($P < 0.001$), a higher preoperative IOP ($P = 0.029$), and a larger preoperative LCCD and BMO width (both $P < 0.001$) were associated with the reduction of the average LCCD (Table 5). Multivariate analysis was performed in two ways to avoid multicollinearity between the preoperative LCCD and preoperative BMO width (variation inflation factor [VIF] = 4.055 and 4.248, respectively). Younger age ($P \leq 0.018$), larger percentage IOP reduction ($P = 0.015$), larger preoperative LCCD ($P < 0.001$), and larger preoperative BMO width ($P < 0.001$) were significantly correlated with the larger LCCD reduction in multivariate analysis (Table 5).

Representative Cases

Three representative cases showing significant reduction of LC curvature after trabeculectomy are presented in Figure 5.

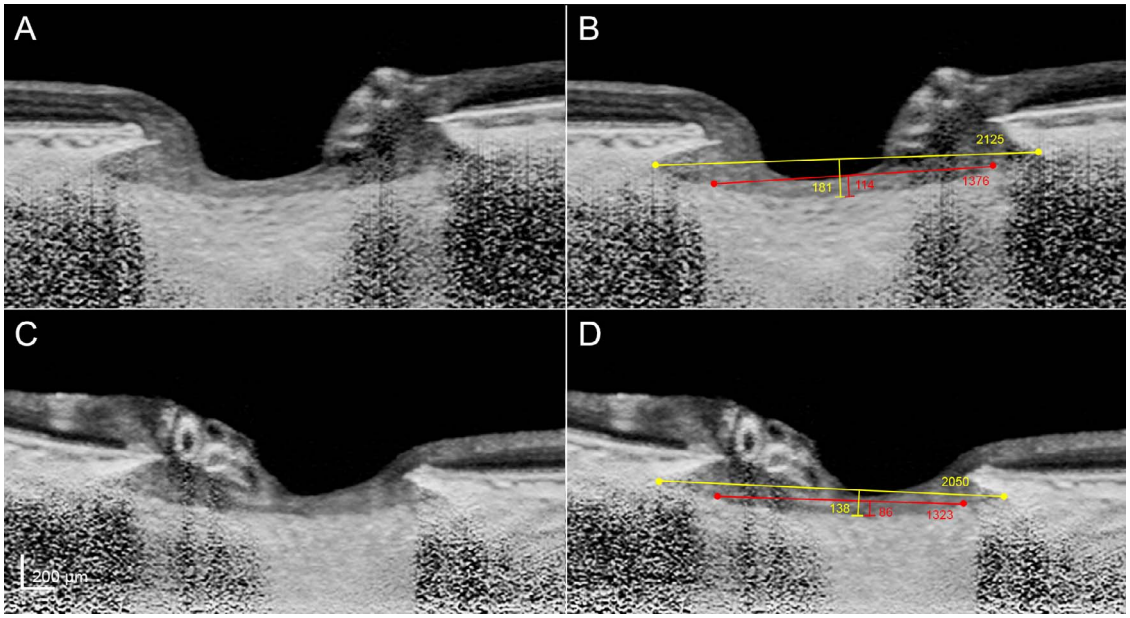

FIGURE 3. Comparison of the curvature of the LC from insertion to insertion and that of the LC within the BMO in two eyes. (**A**, **C**) Images without labeling. (**B**, **D**) Images with labeling. The curvature of the LC from insertion to insertion and that of the LC within the BMO were comparable in both eyes (8.52 vs. 8.28 and 6.73 vs. 6.50, respectively).

TABLE 3. Factors Associated With the Preoperative Lamina Cribrosa Curvature Index

	Superior Midperiphery (Plane 2)				Midhorizontal (Plane 4)				Inferior Midperiphery (Plane 6)			
	Univariate		Multivariate		Univariate		Multivariate		Univariate		Multivariate	
Variables	***β***	***P***	***β***	***P***	***β***	***P***	***β***	***P***	***β***	***P***	***β***	***P***
Age, per 1-year older	**−0.090**	**<0.001**	**−0.076**	**<0.001**	**−0.064**	**0.001**	**−0.055**	**0.004**	**−0.086**	**0.001**	**−0.073**	**0.005**
Sex, female	0.084	0.931			−0.158	0.850			0.604	0.594		
Preoperative IOP, mm Hg	**0.152**	**0.009**	**0.104**	**0.039**	**0.126**	**0.014**	0.091	0.053	**0.179**	**0.010**	**0.133**	**0.039**
Preoperative BMO width, µm	0.002	0.196			0.000	0.852			0.003	0.099	0.002	0.351
AXL, mm	0.164	0.655			0.056	0.857			0.218	0.614		
CCT, µm	0.001	0.950			−0.007	0.994			0.006	0.772		
Global RNFL thickness, µm	−0.003	0.937			−0.003	0.906			−0.003	0.938		
Visual field MD, dB	0.024	0.651			0.039	0.406			0.014	0.827		
Visual field PSD, dB	−0.152	0.243			−0.108	0.336			−0.179	0.246		

Only variables with $P < 0.1$ on univariate analysis were included in the multivariate model. Values with statistical significance are in boldface. BMO, Bruch's membrane opening; AXL, axial length; CCT, central corneal thickness.

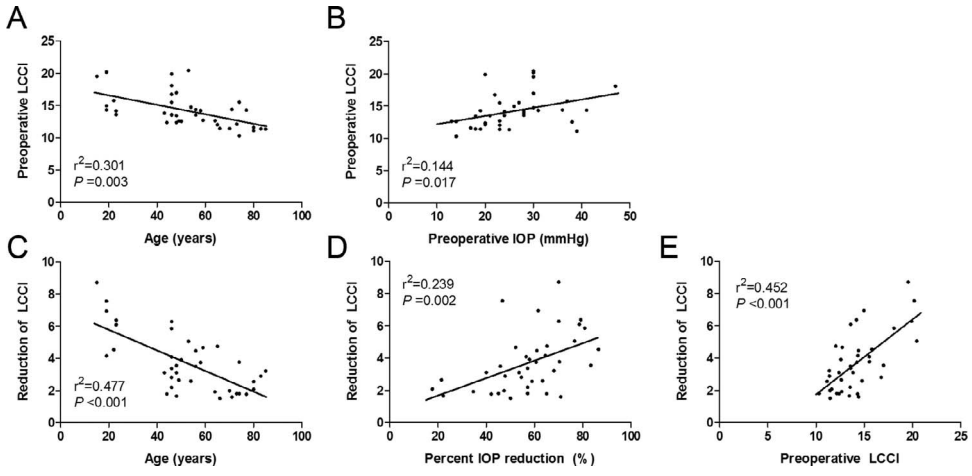

FIGURE 4. Scatter plots showing the relationship between the preoperative LCCI (**A**, **B**) and the reduction of the LCCI (**C**, **D**, **E**), and clinical parameters.

Table 4. Factors Associated With the Reduction of Lamina Cribrosa Curvature Index

	Superior Midperiphery (Plane 2)				Midhorizontal (Plane 4)				Inferior Midperiphery (Plane 6)			
	Univariate		Multivariate		Univariate		Multivariate		Univariate		Multivariate	
Variables	β	P	β	P	β	P	β	P	β	P	β	P
Age, per 1-year older	**−0.080**	**<0.001**	**−0.043**	**0.003**	**−0.062**	**<0.001**	**−0.032**	**0.011**	**−0.069**	**<0.001**	**−0.036**	**0.014**
Sex, female	−0.025	0.973			0.111	0.853			−0.123	0.862		
Preoperative IOP, mm Hg	**0.135**	**0.003**	0.036	0.325	**0.089**	**0.016**	0.026	0.415	**0.129**	**0.003**	0.037	0.342
IOP, % reduction	**0.074**	**<0.001**	**0.038**	**0.017**	**0.048**	**0.005**	0.019	0.166	**0.067**	**0.001**	**0.030**	**0.047**
Preoperative LCCI	**0.559**	**<0.001**	**0.241**	**0.031**	**0.415**	**<0.001**	**0.334**	**0.001**	**0.431**	**<0.001**	**0.325**	**0.005**
Preoperative BMO width, μm	0.002	0.062	0.001	0.118	**0.002**	**0.048**	0.001	0.123	0.002	0.094	0.001	0.240
AXL, mm	0.256	0.435			−0.033	0.882			0.116	0.728		
CCT, μm	0.002	0.816			0.005	0.436			0.011	0.296		
Global RNFL thickness, μm	0.006	0.805			−0.006	0.755			−0.002	0.942		
Visual field MD, dB	0.006	0.883			−0.016	0.630			0.000	0.991		
Visual field PSD, dB	−0.125	0.225			−0.037	0.648			−0.076	0.433		

Only variables with $P < 0.1$ on univariate analysis were included in the multivariate model. Values with statistical significance are in boldface.

Discussion

The present findings demonstrated that the LC curvature is reduced after IOP lowering in glaucomatous eyes. Although the LC depth change has been demonstrated previously, it does not necessarily indicate the LC curvature change because the LC depth change may be attributable to the migration of the LC insertion as a part of active remodeling.[31] To the best of our knowledge, this is the first study to document a reduction of the LC curvature in human glaucomatous eyes in vivo.

The LCCI was measured on horizontal B-scan images because there is horizontal ridge at or near the midhorizontal ONH,[17] and therefore the LC is generally less displaced in this region in both healthy and glaucomatous eyes.[17] This results in a W-shaped curvature of the LC in vertical and oblique scans (i.e., the LC would have two separate curvatures), so that using the vertical or oblique scans would complicate the analysis.

The forces transferred to the LC and that drive its deformations may be diverse. Considering that the posterior bowing of the LC is the principal pathogenic element in glaucoma, the forces can be classified into two categories: (1) the forces that hold the LC flat (e.g., meridional stress in the peripapillary sclera and LC stiffness), and (2) those that cause it to bow posteriorly (e.g., positive TLPD). Based on this classification, a large LC curvature may indicate that the forces causing the posterior bowing of the LC exceed the force that holds the LC flat. This may be attributable to high IOP, low retrolaminar tissue pressure, low meridional tension in the peripapillary sclera, or a combination of those factors. Whatever the cause is, IOP lowering may be adequate in eyes with large LC curvature even if the IOP is low. On the other hand, there is no evidence that chronic IOP-related stress may cause optic nerve damage without inducing LC deformation. In this regard, it is unclear whether IOP-related stress is still the predominant pathogenic factor in eyes with small LC curvature. Even if the IOP is high, a flat LC may indicate that the TLPD is not high (owing to high retrolaminar tissue pressure), or that the effects of the high TLPD on the LC are cancelled off by countering forces. As IOP reduction is the only proven treatment in glaucoma, such classification would not make a big difference in the clinical practice. However, valid subclassification of patients would enhance the understanding of the individual patient's response to the IOP-lowering treatment and facilitate the development of other treatment modalities.

This study was started in a bid to develop a parameter that can be used to assess the mechanical strain in the LC. Since we previously noticed an LC depth change after IOP lowering, we thought LC depth could potentially be considered as a

Table 5. Factors Associated With the Preoperative Average LCCD and the Reduction of Average LCCD

	Preoperative LCCD					Reduction of LCCD						
	Univariate			Multivariate		Univariate			Multivariate1		Multivariate2	
Variables	β	P	VIF	β	P	β	P	VIF	β	P	β	P
Age, per 1-year older	**−1.597**	**0.001**	**1.066**	**−1.045**	**0.001**	**−1.119**	**<0.001**	**1.564**	**−0.377**	**0.018**	**−0.675**	**<0.001**
Sex, female	30.045	0.133				13.608	0.254					
Preoperative IOP, mm Hg	2.283	0.072	1.073	0.123	0.166	**1.625**	**0.029**	1.748	0.213	0.623	0.362	0.412
IOP, % reduction		n/a		n/a		0.664	0.062	1.238	0.182	0.277	**0.438**	**0.015**
Preoperative LCCD, μm		n/a		n/a		**0.526**	**<0.001**	**4.055**	**0.464**	**<0.001**		
Preoperative BMO width, μm	**1.183**	**<0.001**	**1.066**	**0.164**	**<0.001**	**0.105**	**<0.001**	**4.248**			**0.094**	**<0.001**
AXL, mm	0.620	0.932				4.776	0.229					
CCT, μm	−0.065	0.770				0.063	0.610					
Global RNFL thickness, μm	0.341	0.612				0.256	0.520					
Visual field MD, dB	−0.595	0.604				−0.505	0.457					
Visual field PSD, dB	−3.307	0.228				−1.840	0.255					

Only variables with $P < 0.1$ on univariate analysis were included in the multivariate model. Values with statistical significance are in boldface. VIF, variation inflation factor; n/a, not applicable.

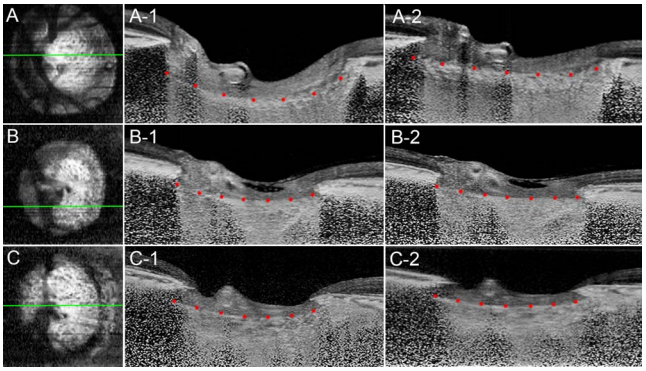

FIGURE 5. Three representative cases. (**A**, **B**, **C**) En face images of the left eye of a 14-year-old female, a 61-year-old male, and a 77-year-old male patient, respectively. (**A-1**, **B-1**, **C-1**) Preoperative B-scan images at the plane indicated by *green line* in the en face images. (**A-2**, **B-2**, **C-2**) B-scan images obtained at postoperative 6 months in the same plane. The intraocular pressure decreased from 26 to 10 mm Hg, 23 to 8 mm Hg, 39 to 16 mm Hg, respectively. Note that the LC curvature was noticeably flattened after trabeculectomy in all three eyes.

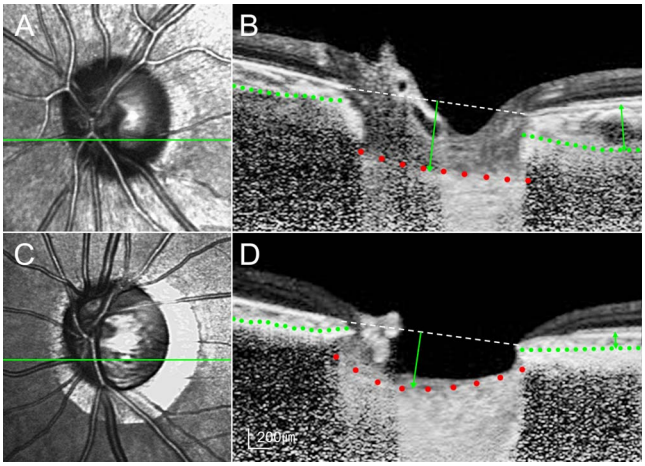

FIGURE 6. Infrared optic disc photograph and B-scan image at the inferior midperiphery of a healthy (**A**, **B**) and a glaucomatous eye (**C**, **D**). *Green dashed line* indicates the approximate sclerochoroidal junction. Healthy eye has greater LC depth (*green arrow*) as measured from the Bruch's membrane opening plane (*white dashed line*). However, the magnitude of posterior LC bowing is greater (*red dots*) in the glaucomatous eye. Note that the peripapillary choroidal thickness (*double headed arrow*) is much larger in the healthy eye. These cases indicate that measuring the LC depth may lead to faulty estimation of the LC strain.

surrogate biomechanical quantity. However, there is a critical limitation to its application. The LC depth is currently measured from the BMO level, and it is largely influenced by the choroidal thickness, which is known to largely vary among individuals.[32,33] For instance, eyes with a thick choroid would have large LC depth even though the LC is not posteriorly curved. In contrast, eyes with a thin choroid would have small LC depth even though the LC is substantially posteriorly bowed (Fig. 6). Another approach for measuring the LC depth while avoiding the influence of choroidal thickness is to measure it from the anterior scleral opening level. However, there is no consensus as to whether the anterior scleral opening can be reliably detected on OCT images. Then, we hypothesized that the LC curve may be another candidate as a parameter relevant with the LC strain. The present study demonstrated that the LC curvature was reduced after the surgery. The LCCI range was less than 13.5 in all eyes postoperatively. We are currently measuring LCCI in healthy eyes. We have found that the LC may be slightly curved in healthy eyes as well, with the average LCCI reaching 12. Thus, it may be considered that postoperatively the LC curvature has returned to, or near to, the level seen in healthy eyes. Taking these factors into consideration, it may be proposed that the LCCI may have value as a parameter that can be used to assess the LC strain.

Previous studies[18,34] have demonstrated that deepening of the LC or no change in the LC depth may also occur after trabeculectomy. In contrast, the LCCI was reduced in all eyes in the present study. We consider that the discrepancy between the LC depth change and the LCCI change is attributable to the change of the choroidal thickness after the surgery. It is known that the choroidal thickness increases after trabeculectomy.[35] The choroidal thickening would increase the LC depth, which is measured from the BMO plane. Thus, if the choroidal thickening is substantial, it may cancel off or surpass the LC depth reduction derived from LC flattening. This would result in increase or no change of LC depth but reduction of LCCI.

The current study evaluated the gross configuration of the LC. While the reduction of IOP, which would lower TLPD, should be relevant to the curvature of the network of the LC beams, several factors such as connective tissue remodeling and collagen rearrangements are also likely to affect the change of curvature 6 months postoperatively. Previous studies[11,36] have demonstrated that the astrocytes and microglia become activated in response to elevated hydrostatic pressure. While it remains unknown how the glial cells respond to decreased hydrostatic pressure, it may be possible that the reduction of the hydrostatic pressure may alter the activity of those cells.

The LCCI was smallest in the midhorizontal plane preoperatively. This finding is consistent with the notion that the LC is less displaced in this region owing to the presence of a horizontal ridge that contains denser fibrous connective tissue than in other regions.[17] In contrast, the superior and inferior regions have a steeper curvature owing to the lower density of connective tissue.[37] It has long been considered that this relatively lower level of connective tissue support is associated with the preferential occurrence of glaucomatous optic nerve damage at the superior and inferior regions of the optic nerve.[38]

Larger IOP reduction, younger age, and larger preoperative LCCI were associated with a larger reduction of the LCCI. This finding is in line with a previous observation of reduction of the LC depth after IOP lowering, in which younger age, larger baseline LC displacement, and larger IOP reduction are associated with the LC depth reduction after trabeculectomy.[18,34] The significant influence of age on the LCCI change indicates that mechanical properties of the LC tissue may be another important factor influencing the LC curve change other than TLPD.

The findings of this study should be considered in light of its limitations. First, for precise quantification of curvature, a reference line should be measured from the LC insertion. However, only the LC within the BMO width was included for measuring the LC curvature in the present study. This was because the LC was often not visible outside of this region. Nonetheless, in eyes in which the LC was visible up to the LC insertion, the LCCI measured from the whole LC (between the LC insertions) was comparable with that measured on the LC within the BMO. Thus, we consider that the curvature of the LC assessed within the BMO may be used as a surrogate for the actual LC curvature. Second, we referred to the change in the LC configuration as a change in curvature. However, the

curvature is a geometric entity that refers to the inverse of the radius of the arc of a circle best fitting the portion of the curve. Thus, it should be considered that the LCCI is not a parameter corresponding to an actual LC curvature. Third, measurements were obtained manually, not using an automated algorithm, which could have produced observer-related bias. Fourth, the current study included only Korean patients; it is not known whether the present findings can be extrapolated to other ethnic populations.

In conclusion, LC curvature was reduced after IOP lowering. This finding suggests that LC curvature may have value as a parameter relevant to ONH biomechanics. Further study is needed to determine the validity and usefulness of LC curvature for evaluation of the LC strain.

Acknowledgments

Supported by the National Research Foundation of Korea Grant, funded by the Korean Government (Grant No. 2013R1A1A1A05004781), Seoul, Korea. The funding organization had no role in the design or conduct of this research.

Disclosure: **S.H. Lee**, None; **D.-A. Yu**, None; **T.-W. Kim**, Topcon (C); **E.J. Lee**, None; **M.J.A. Girard**, None; **J.M. Mari**, None

References

1. Leske MC, Connell AM, Wu SY, Hyman LG, Schachat AP. Risk factors for open-angle glaucoma: The Barbados Eye Study. *Arch Ophthalmol*. 1995;113:918–924.
2. Burgoyne CF, Downs JC, Bellezza AJ, Suh JK, Hart RT. The optic nerve head as a biomechanical structure: a new paradigm for understanding the role of IOP-related stress and strain in the pathophysiology of glaucomatous optic nerve head damage. *Prog Retin Eye Res*. 2005;24:39–73.
3. Kass MA, Heuer DK, Higginbotham EJ, et al. The Ocular Hypertension Treatment Study: a randomized trial determines that topical ocular hypotensive medication delays or prevents the onset of primary open-angle glaucoma. *Arch Ophthalmol*. 2002;120:701–713, discussion 829–830.
4. Medeiros FA, Weinreb RN, Sample PA, et al. Validation of a predictive model to estimate the risk of conversion from ocular hypertension to glaucoma. *Arch Ophthalmol*. 2005; 123:1351–1360.
5. Gordon MO, Beiser JA, Brandt JD, et al. The Ocular Hypertension Treatment Study: baseline factors that predict the onset of primary open-angle glaucoma. *Arch Ophthalmol*. 2002;120:714–720, discussion 829–830.
6. Sommer A, Tielsch JM, Katz J, et al. Relationship between intraocular pressure and primary open angle glaucoma among white and black Americans: The Baltimore Eye Survey. *Arch Ophthalmol*. 1991;109:1090–1095.
7. Heijl A, Leske MC, Bengtsson B, Hyman L, Bengtsson B, Hussein M. Reduction of intraocular pressure and glaucoma progression: results from the Early Manifest Glaucoma Trial. *Arch Ophthalmol*. 2002;120:1268–1279.
8. Bellezza AJ, Hart RT, Burgoyne CF. The optic nerve head as a biomechanical structure: initial finite element modeling. *Invest Ophthalmol Vis Sci*. 2000;41:2991–3000.
9. Yan DB, Coloma FM, Metheetrairut A, Trope GE, Heathcote JG, Ethier CR. Deformation of the lamina cribrosa by elevated intraocular pressure. *Br J Ophthalmol*. 1994;78:643–648.
10. Sigal IA, Flanagan JG, Tertinegg I, Ethier CR. Predicted extension, compression and shearing of optic nerve head tissues. *Exp Eye Res*. 2007;85:312–322.
11. Downs JC, Roberts MD, Burgoyne CF. Mechanical environment of the optic nerve head in glaucoma. *Optom Vis Sci*. 2008;85: 425–435.
12. Sigal IA, Flanagan JG, Tertinegg I, Ethier CR. Modeling individual-specific human optic nerve head biomechanics, part I: IOP-induced deformations and influence of geometry. *Biomech Model Mechanobiol*. 2009;8:85–98.
13. Hernandez MR, Miao H, Lukas T. Astrocytes in glaucomatous optic neuropathy. *Prog Brain Res*. 2008;173:353–373.
14. Campbell IC, Coudrillier B, Ross Ethier C. Biomechanics of the posterior eye: a critical role in health and disease. *J Biomech Eng*. 2014;136:021005.
15. Girard MJ, Strouthidis NG, Desjardins A, Mari JM, Ethier CR. In vivo optic nerve head biomechanics: performance testing of a three-dimensional tracking algorithm. *J R Soc Interface*. 2013; 10:20130459.
16. Girard MJ, Dupps WJ, Baskaran M, et al. Translating ocular biomechanics into clinical practice: current state and future prospects. *Curr Eye Res*. 2015;40:1–18.
17. Park SC, Kiumehr S, Teng CC, Tello C, Liebmann JM, Ritch R. Horizontal central ridge of the lamina cribrosa and regional differences in laminar insertion in healthy subjects. *Invest Ophthalmol Vis Sci*. 2012;53:1610–1616.
18. Lee EJ, Kim TW, Weinreb RN. Reversal of lamina cribrosa displacement and thickness after trabeculectomy in glaucoma. *Ophthalmology*. 2012;119:1359–1366.
19. Lee EJ, Kim TW, Weinreb RN. Variation of lamina cribrosa depth following trabeculectomy. *Invest Ophthalmol Vis Sci*. 2013;54:5392–5399.
20. Lee EJ, Kim TW, Weinreb RN, Kim H. Reversal of lamina cribrosa displacement after intraocular pressure reduction in open-angle glaucoma. *Ophthalmology*. 2013;120:553–559.
21. Seo JH, Kim TW, Weinreb RN. Lamina cribrosa depth in healthy eyes. *Invest Ophthalmol Vis Sci*. 2014;55:1241–1251.
22. Rhodes LA, Huisingh C, Johnstone J, et al. Peripapillary choroidal thickness variation with age and race in normal eyes. *Invest Ophthalmol Vis Sci*. 2015;56:1872–1879.
23. Lee EJ, Kim TW, Weinreb RN. Improved reproducibility in measuring the laminar thickness on enhanced depth imaging SD-OCT images using maximum intensity projection. *Invest Ophthalmol Vis Sci*. 2012;53:7576–7582.
24. Lee EJ, Kim TW, Weinreb RN, Park KH, Kim SH, Kim DM. Visualization of the lamina cribrosa using enhanced depth imaging spectral-domain optical coherence tomography. *Am J Ophthalmol*. 2011;152:87–95, e81.
25. Kim YW, Lee EJ, Kim TW, Kim M, Kim H. Microstructure of beta-zone parapapillary atrophy and rate of retinal nerve fiber layer thinning in primary open-angle glaucoma. *Ophthalmology*. 2014;121:1341–1349.
26. Choi YJ, Lee EJ, Kim BH, Kim TW. Microstructure of the optic disc pit in open-angle glaucoma. *Ophthalmology*. 2014;121: 2098–2106.
27. Jonas JB, Kling F, Grundler AE. Optic disc shape, corneal astigmatism, and amblyopia. *Ophthalmology*. 1997;104:1934–1937.
28. Spaide RF, Koizumi H, Pozonni MC. Enhanced depth imaging spectral-domain optical coherence tomography. *Am J Ophthalmol*. 2008;146:496–500.
29. Girard MJ, Strouthidis NG, Ethier CR, Mari JM. Shadow removal and contrast enhancement in optical coherence tomography images of the human optic nerve head. *Invest Ophthalmol Vis Sci*. 2011;52:7738–7748.
30. Mari JM, Strouthidis NG, Park SC, Girard MJ. Enhancement of lamina cribrosa visibility in optical coherence tomography images using adaptive compensation. *Invest Ophthalmol Vis Sci*. 2013;54:2238–2247.
31. Yang H, Williams G, Downs JC, et al. Posterior (outward) migration of the lamina cribrosa and early cupping in monkey experimental glaucoma. *Invest Ophthalmol Vis Sci*. 2011;52: 7109–7121.

32. Johnstone J, Fazio M, Rojananuangnit K, et al. Variation of the axial location of Bruch's membrane opening with age, choroidal thickness, and race. *Invest Ophthalmol Vis Sci*. 2014;55:2004–2009.
33. Rhodes LA, Huisingh C, Johnstone J, et al. Variation of laminar depth in normal eyes with age and race. *Invest Ophthalmol Vis Sci*. 2014;55:8123–8133.
34. Reis AS, O'Leary N, Stanfield MJ, Shuba LM, Nicolela MT, Chauhan BC. Laminar displacement and prelaminar tissue thickness change after glaucoma surgery imaged with optical coherence tomography. *Invest Ophthalmol Vis Sci*. 2012;53:5819–5826.
35. Saeedi O, Pillar A, Jefferys J, Arora K, Friedman D, Quigley H. Change in choroidal thickness and axial length with change in intraocular pressure after trabeculectomy. *Br J Ophthalmol*. 2014;98:976–979.
36. Hernandez MR. The optic nerve head in glaucoma: role of astrocytes in tissue remodeling. *Prog Retin Eye Res*. 2000;19:297–321.
37. Radius RL. Regional specificity in anatomy at the lamina cribrosa. *Arch Ophthalmol*. 1981;99:478–480.
38. Quigley HA, Addicks EM. Regional differences in the structure of the lamina cribrosa and their relation to glaucomatous optic nerve damage. *Arch Ophthalmol*. 1981;99:137–143.

Investigative Ophthalmology & Visual Science